

randomized into six treatment groups (13 mice in each group): ZOL, SMS, SOM, ZOL plus SMS, ZOL plus SOM, and control. The groups were treated for 6 weeks with ZOL (1 $\mu\text{g}/\text{mouse}$, three times per week, s.c.), SMS (2 $\mu\text{g}/\text{mouse}$, once per day, s.c.), SOM (2 $\mu\text{g}/\text{mouse}$, twice per day, s.c.), ZOL plus SMS (1 $\mu\text{g}/\text{mouse}$, three times per week, s.c. plus 2 $\mu\text{g}/\text{mouse}$, once per day, s.c.), ZOL plus SOM (1 $\mu\text{g}/\text{mouse}$, three times per week, s.c. plus 2 $\mu\text{g}/\text{mouse}$, twice per day, s.c.), or saline (an equal volume of solvent/day, s.c.). These substances were dissolved in 100 μl saline. ZOL, SMS, and SOM were kindly provided by Novartis Pharma AG (Basel, Switzerland). These agents were soluble in saline. The body weights of mice were measured each week. The effects of treatments on tumor growth were determined by measuring tumor volume ($0.523 \times \text{long diameter}^2 \times \text{short diameter}$). After 6 weeks of treatment, the mice were killed and the tumor and liver were removed. Liver weight was measured, and the numbers of metastatic nodules on the liver surface were macroscopically counted. The tissues were fixed in 10% formalin and embedded in paraffin. The 5 μm thick paraffin-embedded material was routinely processed for hematoxylin and eosin staining.

The Animal Experiment Committee of Sapporo Medical University approved the *in vivo* experiments. Animal care and housing followed the guidelines of the Animal Experiment Committee.

Cell Cycle and Apoptosis Analysis of Tissue Sections

Immunohistochemical staining was done with formalin-fixed paraffin-embedded tissue sections of NE-10 tumors. The 5 μm thick sections were deparaffinized in xylene and rehydrated in graded alcohol. Antigen retrieval was done by boiling sections for 20 min in a microwave oven in preheated 0.01 mol/L sodium citrate buffer (pH 6.0). Endogenous peroxidase activity was blocked by 3% hydrogen peroxide in ethanol for 10 min. After blocking with 1% non-fat dry milk in phosphate-buffered saline (PBS) (pH 7.4), the sections were reacted with a rabbit polyclonal anti-Ki-67 antibody (Abcam plc., Cambridge, UK) at 20 $\mu\text{g}/\text{ml}$ or preimmune sera for 1 hr, followed by incubation with biotinylated goat anti-rabbit IgG (Nichirei, Tokyo, Japan) for 30 min. Subsequently, the sections were stained with streptavidin-biotin complex (Nichirei), followed by incubation with 3,3'-diaminobenzidine and counterstaining with hematoxylin. The same tissues were immunostained by TdT-mediated dUTP-biotin nick-end labeling (TUNEL) (In situ Apoptosis Detection Kit, Takara Bio, Inc., Otsu, Japan). The Ki-67 labeling index (KI) and apoptotic

index (AI) were determined as the ratios of immunohistochemically positive cells per 1,000 NE cells by using a fluorescence microscope (model BZ-9000; Keyence, Osaka, Japan).

Proliferation Assays

NE-CS cells (1×10^4) were suspended with 100 μl of culture medium in a 96-well plate for 24 hr, and then treated with the indicated concentrations (from 0.1 to 100 $\mu\text{mol}/\text{L}$) of ZOL, SMS and SOM for 24, 48, or 72 hr. For combination, the same concentrations of ZOL and SMS or SOM were used; for example, 1 $\mu\text{mol}/\text{L}$ of ZOL to 1 $\mu\text{mol}/\text{L}$ of SMS. In addition, they were treated with the indicated concentrations (from 0.1 to 100 $\mu\text{mol}/\text{L}$) of ZOL plus 1, 5, and 20 $\mu\text{mol}/\text{L}$ of farnesyl-pyrophosphate ammonium salt (FOH) (Sigma-Aldrich, St. Louis, MO) for 48 hr. FOH is an isoprenoid to be involved in prenylation of several G proteins including Ras in the intracellular mevalonate pathway. Cell proliferation was assessed using a WST-8 (modified tetrazolium salt) cell proliferation kit (Cell Counting Kit-8, Dojin, Japan). Changes in absorbance at 450 nm were measured with a microplate reader. The growth inhibition was determined as the concentration inducing 50% inhibition (IC₅₀). For analysis of the synergism between ZOL and somatostatin analogs (SMS and SOM), the combination indices (CI) were calculated by the isobologram equation method [18,19], and CI values of <1, 1, and >1 were considered to indicate synergistic, additive, and antagonistic effects, respectively [12].

Cell Cycle and Apoptosis Assays

NE-CS cells (3×10^4) were suspended with 100 μl of culture medium in a 96-well plate for 24 hr, and then treated with various concentrations of ZOL (from 10 to 100 $\mu\text{mol}/\text{L}$) for 48 hr. Then the cells were fixed with 4% paraformaldehyde, permeabilized with 0.1% Triton X-100, and labeled with the TUNEL technique (In situ Cell Death Detection Kit TMR red, Roche Diagnostics, Mannheim, Germany) and the primary anti-Ki-67 antibody at a 1/200 dilution (Abcam plc., Cambridge, UK). The Ki-67 antibody was detected with an Alexa Fluor 488 donkey anti-rabbit antibody, and nuclei were stained with 4,6-diamidino-2-phenylindole (DAPI) (Invitrogen, Carlsbad, CA). As in the *in vivo* study, the KI and the AI were measured by fluorescence immunohistochemistry using a fluorescence microscope (model BZ-9000; Keyence, Osaka, Japan).

Migration Assays

Cell migration analyses were performed as described previously (10). In a trans-well culture

chamber (Coster Science, Cambridge, MA), a polyvinylpyrrolidone-free polycarbonate filter with an 8.0 μm pore size was precoated with 5 μg of fibronectin (Biomedical Technologies, Stoughton, MA) on the lower surface. Two different experiments were performed. In experiment 1, NE-CS cells (1×10^5) were placed in the upper chamber with 100 μl of culture medium with or without ZOL (10, 100 $\mu\text{mol/L}$). In the lower chamber, 600 μl of culture medium was added. In experiment 2, NE-CS cells (1×10^5) were placed in the upper chamber with 100 μl of culture medium adding 20 $\mu\text{mol/L}$ of FOH with or without ZOL (10, 100 $\mu\text{mol/L}$). In the lower chamber, 600 μl of culture medium was added. The cells that migrated across the pores at 2, 4, 6, and 8 hr were counted under a microscope after hematoxylin and eosin staining. The experiments were carried out in triplicate. Data are shown as number of cells 1 mm^2 of membrane.

Pull Down and Western Blot Assays

NE-CS cells (1×10^5) were suspended with 2 ml of culture medium in a 6-well plate for 24 hr, and then treated with ZOL (10, 100 $\mu\text{mol/L}$) or ZOL (10, 100 $\mu\text{mol/L}$) + 20 $\mu\text{mol/L}$ FOH for 48 hr. Subsequent to the treatment, cells were washed three times with ice-cold PBS and solubilized in lysis buffer [RIPA buffer, 100 mmol/L PMSF, 500 mmol/L Na_3VO_4 , 1 mol/L NaF, 2 mol/L Sigma 104 phosphatase substrate, Protease Inhibitor Mini Cocktail]. The total protein content of the cell lysates was determined by the BCA Protein Assay (Pierce, Rockford, IL).

Activated Ras was detected by pull-down assay. The GTP-bound form of Ras in the cell lysates was affinity-purified using the Raf1-Ras-binding domain (RBD)-GST complexed with glutathione beads following the manufacturer's instructions (Active Ras Pull Down and Detection Kit, Thermo Fisher Science, Waltham, MA). Complexes were analyzed by SDS-PAGE and immunoblotting with a Ras-specific antibody.

The cells lysates obtained were boiled in SDS sample buffer containing 0.5 mol/L 2-mercaptoethanol. Samples were separated by SDS-PAGE, transferred to polyvinylidene difluoride (PVDF) membranes and immunoblotted with rabbit monoclonal anti-Erk1/2 and anti-phospho-Erk1/2 antibodies (Cell Signaling Technology Inc., MA), and a mouse monoclonal anti- β -actin antibody (Sigma-Aldrich). Separated proteins were visualized using horseradish peroxidase with enhancement by chemiluminescence (GE Healthcare Bio-Sciences Corp., NJ).

Statistical Analysis

We used the computer program StatView 5.0 for Windows (SAS Institute, Cary, NC). Student's *t*-test

was applied to compare results between two different groups. Repeated-measures ANOVA was used when comparing the in vivo tumor volume, and the in vitro cell migration in an individual group. One-way ANOVA was used when comparing the in vivo apoptosis, cell cycle progression, and liver metastases in an individual group. Statistical significance was assigned at $P < 0.05$.

RESULTS

Expression of SSTR2a and SSTR5 in NE-10 Allografts

Since effects of somatostatin analogs are mediated by expression of SSTR, we examined expression of the somatostatin receptor subtypes SSTR2 and SSTR5, to which SMS and SOM preferentially bind, respectively. Gene expression of SSTR2a and SSTR5 was observed in NE-10 allografts, but that of SSTR2b was not (Fig. 1).

Effects of ZOL, SMS and SOM as Single Agents and in Combination on Subcutaneously Inoculated NE-10 Allografts

Growth of NE-10 tumors in mice treated with ZOL, ZOL plus SMS, and ZOL plus SOM was significantly slowed compared to the saline control ($P = 0.003$, $P < 0.001$, and $P = 0.001$, respectively) (Fig. 2A). All treatments were well tolerated with maintenance of body weight (data not shown). We examined whether anti-tumor effects of each treatment were induced by apoptosis or cell cycle arrest by using TUNEL and Ki67 staining, respectively (Fig. 2B₁). The AI was significantly increased in tumors of mice treated with ZOL, ZOL plus SMS, or ZOL plus SOM compared to the control (means: 9.2, 11.6, and 12.7, respectively, vs. 2.4) (Fig. 2B₂). The KI was significantly decreased in tumors of mice treated with ZOL, ZOL plus SMS, or ZOL plus SOM compared to the control (means: 5.3, 8.3, and 4.2, respectively, vs. 15.9) (Fig. 2B₃). The

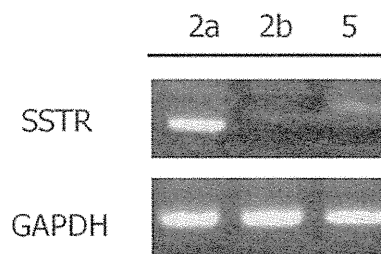


Fig. 1. Expression of SSTR2a, SSTR2b, and SSTR5 in NE 10 allograft by RT PCR. Gene expression of SSTR2a, and SSTR5 was observed in the NE 10 allograft, but that of SSTR2b was not.

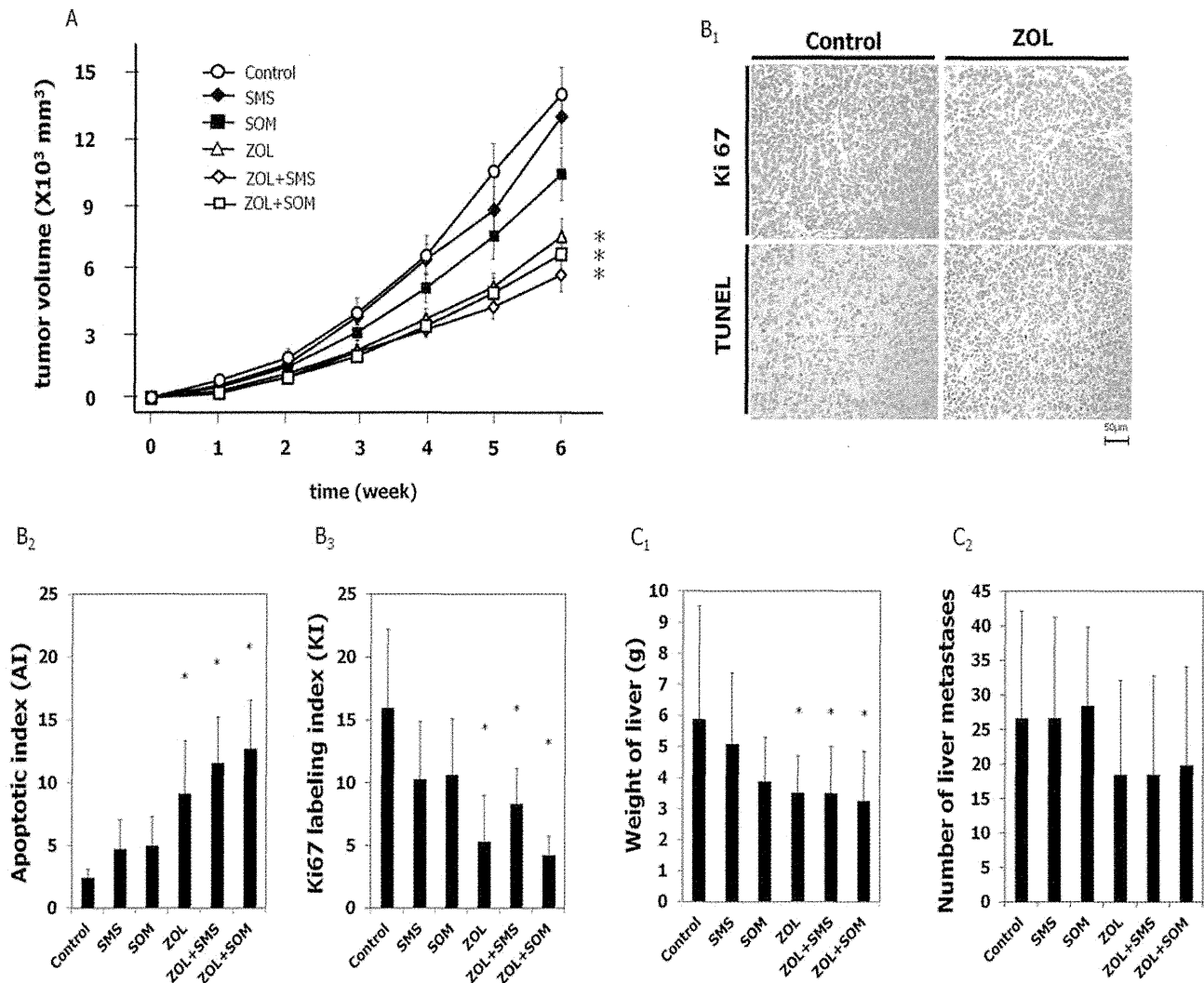


Fig. 2. Effects of ZOL, SMS, and SOM as single agents and in combination on subcutaneous inoculated NE 10 allografts. Six week old male BALB/c nude mice were castrated. After one week, 50 mg tissue fragments from the NE 10 allograft model were subcutaneously inoculated into the backs of mice. For 2 weeks, NE 10 tumors were allowed to grow to approximately more than 100 mm³ before randomization into six treatment groups: control, ZOL, SMS, SOM, ZOL plus SMS, and ZOL plus SOM (n = 13/group). NE 10 allografts in each group were treated for 6 weeks. **A:** Growth of NE 10 tumors in mice treated with ZOL, ZOL plus SMS, and ZOL plus SOM was significantly slowed compared to the saline control (P = 0.003, P < 0.001, and P = 0.001, respectively). Data are means; bars ± SE; *, significantly different from control group (P < 0.05; repeated measures ANOVA). **B:** Effects of ZOL, SMS and SOM as single agents and in combination on apoptosis and cell cycle progression. Immunohistochemical staining was done by using TUNEL and Ki67 staining (**B₁**). Apoptotic effects were measured by the number of TUNEL positive cells per 1,000 cells, apoptotic index (AI). The AI was significantly increased in tumors from mice treated with ZOL, ZOL plus SMS, or ZOL plus SOM compared to the control (means: 9.2, 11.6, and 12.7, respectively, vs. 2.4) (**B₂**). Cell cycle progression was measured by the number of Ki67 positive cells per 1,000 cells (KI: Ki 67 labeling index). The KI was significantly decreased in tumors from mice treated with ZOL, ZOL plus SMS, or ZOL plus SOM compared to the control (means: 5.3, 8.3, and 4.2, respectively, vs. 15.9) (**B₃**). Data are means; bars ± SD; *, significantly different from control group (P < 0.05; one way ANOVA). **C:** Effects of ZOL, SMS and SOM as single agents and in combination on liver metastases. The weights of livers having metastatic nodules in ZOL, ZOL plus SMS, or ZOL plus SOM were significantly lower than for the control (**C₁**), but the numbers of metastatic nodules in these groups were not significantly different from the control (**C₂**). Data are means; bars ± SD. *, Significantly different from control group (P < 0.05; one way ANOVA).

weights of livers having metastatic nodules in ZOL, ZOL plus SMS, or ZOL plus SOM were significantly lower than for the control (Fig. 2C₁), but the numbers of metastatic nodules in these groups were not significantly different from the control (Fig. 2C₂).

Effects of ZOL, SMS and SOM as Single Agents and in Combination on Growth of NE-CS Cells In Vitro

We investigated the inhibitory effects of ZOL, SMS, and SOM, alone and in combination, on proliferation

of NE-CS cells. Cell viability was measured by the WST-8 assay when NE-CS cells were treated with various concentrations of ZOL, SMS and SOM (0.1–100 $\mu\text{mol/L}$) in the treatment groups for 24, 48 or 72 hr. For combinations, the same concentrations of ZOL and SMS or SOM were used. The IC₅₀ for ZOL at 72 hr was 15.7 $\mu\text{mol/L}$, whereas those for ZOL plus SMS, and ZOL plus SOM were 14.1, and 13.5 $\mu\text{mol/L}$, respectively (Fig. 3A). The combination of ZOL and somatostatin analogs did not demonstrate synergistic effects (CI: 0.57–1.00). ZOL induced time-

and dose-dependent proliferative inhibition of NE-CS cells (Fig. 3B). These effects of ZOL were reversed by 20 $\mu\text{mol/L}$ of FOH (Fig. 3C).

ZOL Inhibits Cell Cycle Activity and Induces Apoptosis of NE-CS Cells

TUNEL-positive cells, indicated in red, increased with increased concentrations of ZOL. On the other hand, Ki-67-positive cells, colored green, decreased (Fig. 4A). We also analyzed the AI and KI with ZOL

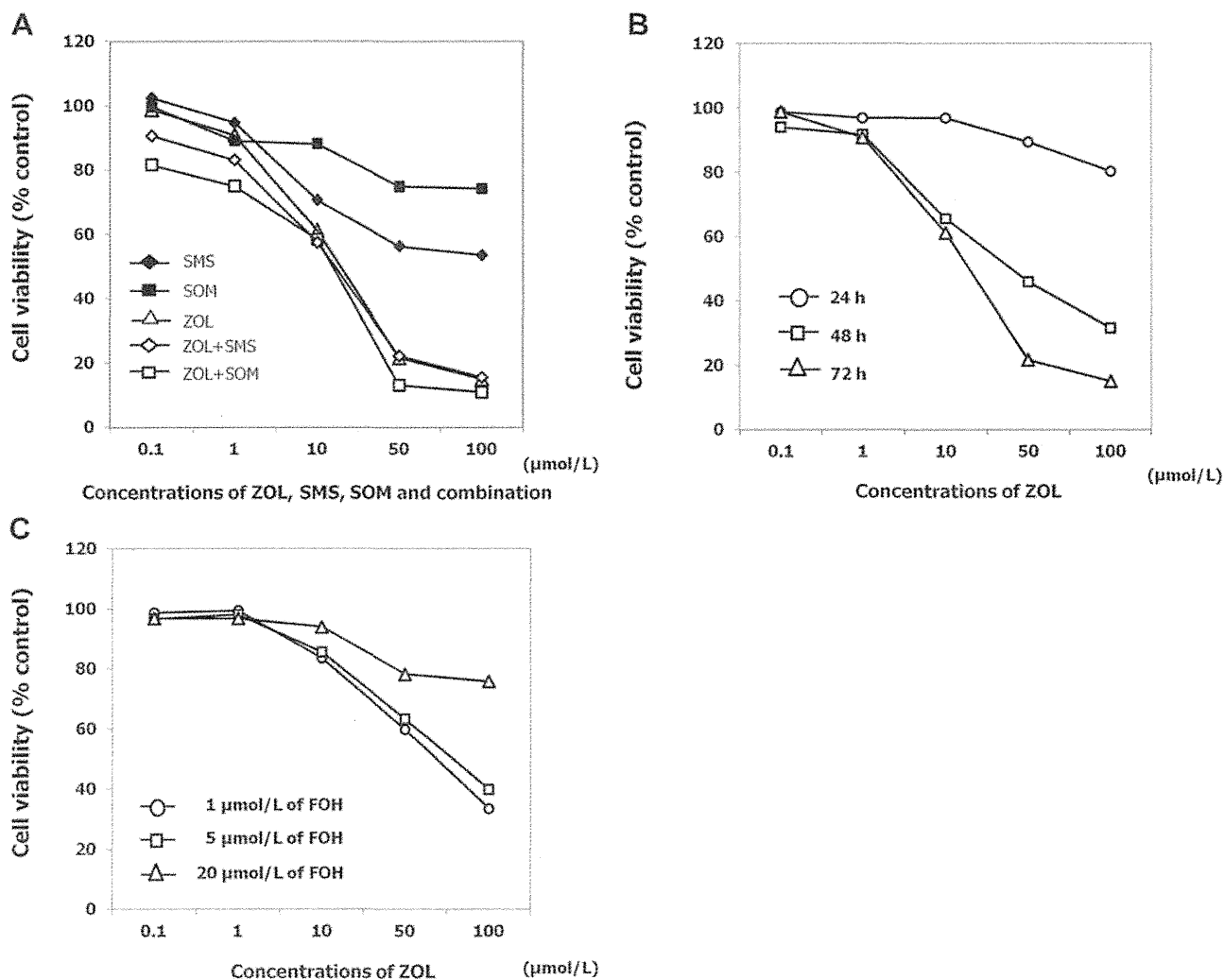


Fig. 3. Effects of ZOL, SMS and SOM as single agents and in combination on growth of NE CS cells. Cell viability was measured by WST 8 assay when NE CS cells were treated with various concentrations of ZOL, SMS and SOM (0.1–100 $\mu\text{mol/L}$) for 24, 48 or 72 hr. For combination, the same concentrations of ZOL and SMS or SOM were used. Cell viability was also measured when NE CS cells were treated for 48 hr with the indicated concentrations (from 0.1 to 100 $\mu\text{mol/L}$) of ZOL plus 1, 5, and 20 $\mu\text{mol/L}$ of farnesyl pyrophosphate ammonium salt (FOH) ($n = 5/\text{group}$). **A:** Cell viability of NE CS cells at 72 hr in each treatment group. The IC₅₀ of ZOL at 72 hr for NE CS cells was 15.7 $\mu\text{mol/L}$ for ZOL, whereas it was 14.1 $\mu\text{mol/L}$ for ZOL plus SMS, and 13.5 $\mu\text{mol/L}$ for ZOL plus SOM. The combination of ZOL and somatostatin analogs did not create synergistic effects. **B:** Cell viability of NE CS cells in time and dose dependent manners. ZOL induced time and dose dependent proliferative inhibition of NE CS cells. **C:** Cell viability of NE CS cells at 48 hr in ZOL plus FOH. ZOL induced inhibition was reversed by 20 $\mu\text{mol/L}$ of FOH.

concentrations of 0, 10, 50, and 100 $\mu\text{mol/L}$. The AI was significantly increased in ZOL 50, and 100 $\mu\text{mol/L}$ compared to the control (means: 55.7 and 136.5, respectively, vs. 13.8) (Fig. 4B). The KI was significantly decreased in ZOL 10, 50, and 100 $\mu\text{mol/L}$ compared to the control (means: 37.6, 22.8, and 1.3, respectively, vs. 68.7) (Fig. 4C).

ZOL Inhibits Migration of NE-CS Cells

In addition to effects of ZOL on cell cycle activity and apoptosis, we examined whether ZOL inhibited migration of NE-CS cells, using a Boyden chamber assay. NE-CS cells, with or without ZOL concentrations of 10, and 100 $\mu\text{mol/L}$, that migrated across the pores at 2, 4, 6 and 8 hr were counted. The numbers of cells migrating 1 mm^2 of membrane were significantly decreased in ZOL 10, and 100 $\mu\text{mol/L}$ (Fig. 5A). When culture medium adding 20 $\mu\text{mol/L}$ of FOH

was incubated in upper chamber, the ZOL-induced inhibition was not appeared (Fig. 5B).

ZOL Utilizes the Ras/MAPK Pathway via the Mevalonate Pathway in NE-CS Cells

Since ZOL inhibits farnesyl-pyrophosphate synthetase in the mevalonate pathway and impairs prenylation of Ras, we evaluated the effects of ZOL on Ras activity. We used FOH, which potentially induces farnesylation of Ras. As evaluated by pull-down assay, 10, and 100 $\mu\text{mol/L}$ inhibited Ras activation in NE-CS cells, and then the ZOL-induced inhibition was reversed by FOH (Fig. 6). We examined the effects of ZOL on Erk-1/2, which are the terminal proteins of the Ras/MAPK pathway. ZOL inhibited Erk1/2 phosphorylation as evaluated by Western blot assay.

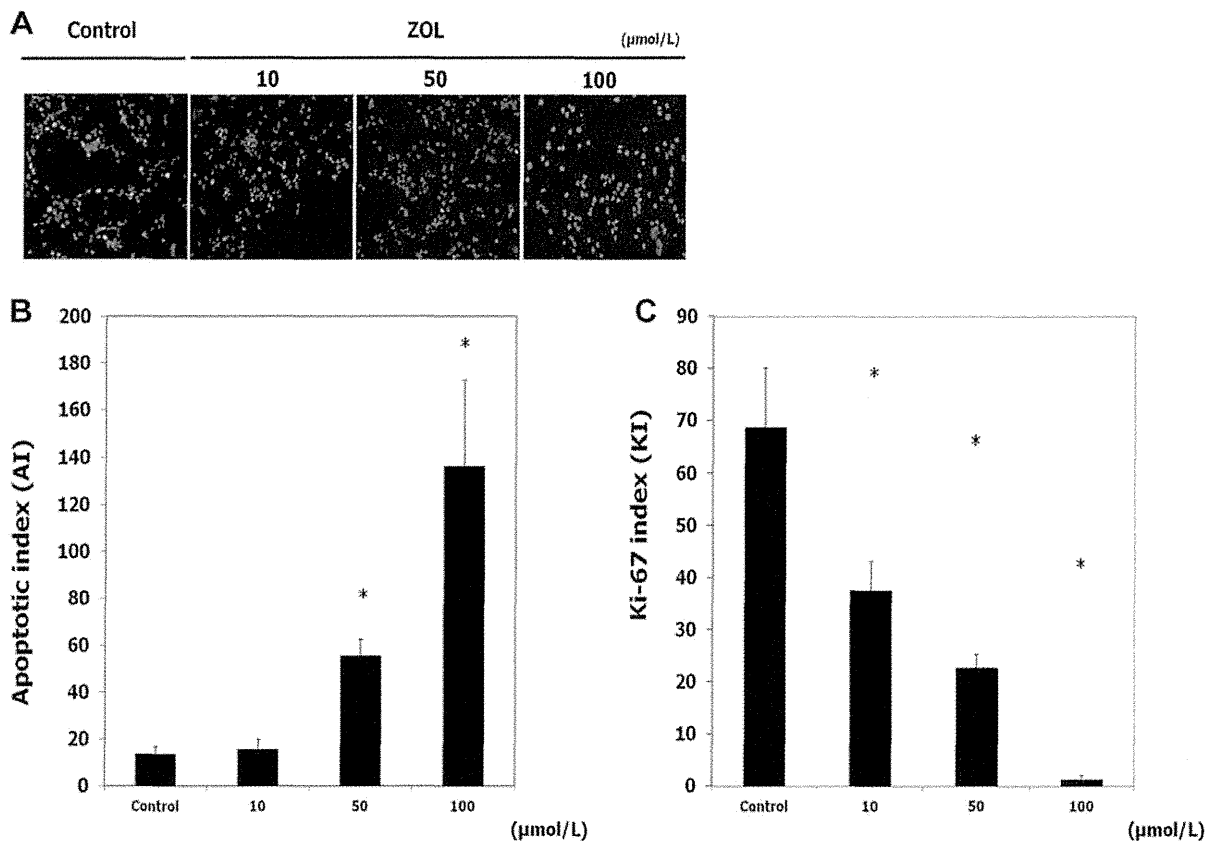


Fig. 4. Effects of ZOL on apoptosis and cell activity of NE-CS cells. **A:** TUNEL and anti Ki67 immunofluorescence were used for NE-CS cells treated with ZOL concentrations of 0, 10, 50, and 100 $\mu\text{mol/L}$ ($n = 5/\text{group}$). DAPI was used to visualize cell nuclei. TUNEL positive cells, colored red, increased with increased concentrations of ZOL. On the other hand, Ki 67 positive cells, colored green, decreased. **B:** The numbers of TUNEL positive cells per 1,000 cells apoptotic index (AI) were significantly increased in ZOL 50, and 100 $\mu\text{mol/L}$ compared to the control (means: 55.7, and 136.5, respectively, vs. 13.8). Data are means; bars \pm SD; *, significantly different from control group ($P < 0.001$; Student's t test). **C:** The numbers of Ki67 positive cells per 1,000 cells (KI: Ki 67 labeling index) were significantly decreased in ZOL 10, 50, and 100 $\mu\text{mol/L}$ compared to the control (means: 37.6, 22.8, and 1.3, respectively, vs. 68.7). Data are means; bars \pm SD; *, significantly different from control group ($P < 0.001$; Student's t test).

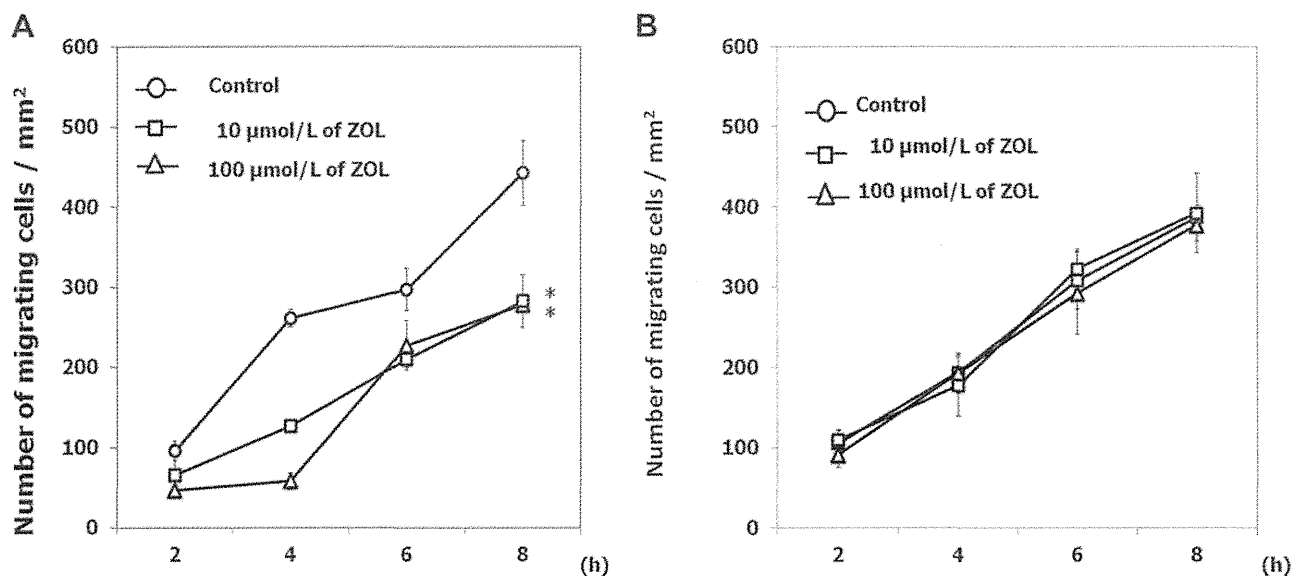


Fig. 5. Effects of ZOL on migration of NE CS cells. Migration assay was performed by using a Boyden chamber (n = 3/group). **A:** In experiment 1, NE CS cells (1×10^5) were placed in the upper chamber with 100 μ l of culture medium with or without ZOL (10, 100 μ mol/L). In the lower chamber, 600 μ l of culture medium was added. The numbers of cells migrating per 1 mm^{-2} of membrane were significantly decreased in ZOL 10, and 100 μ mol/L. Data are means; bars \pm SD; *, significantly different from the control ($P < 0.001$; repeated measures ANOVA). **B:** In experiment 2, culture medium adding 20 μ mol/L of farnesyl pyrophosphate ammonium salt (FOH) was incubated in the upper chamber. The numbers of cells migrating 1 mm^{-2} of membrane were not significantly decreased in ZOL 10, and 100 μ mol/L. Data are means; bars \pm SD. *, Significantly different from the control ($P < 0.001$; repeated measures ANOVA).

DISCUSSION

Inappropriate NE regulation in the prostate might facilitate carcinogenesis, proliferation and other tissue changes such as loss of basal cells, angiogenesis, and piling up of prostatic luminal epithelium and invasion, which are characteristic of prostatic carcinoma

[20]. In addition, we previously demonstrated that secretions from NE cells stimulated prostatic cancer cells to achieve androgen-independent growth [21]. Androgen deprivation therapy induces an increased number of NE cells in prostate cancer and the frequency and density of NE cells are more pronounced in CRPC [22]. Thus, the control of NE cells might be important for establishing a treatment strategy for CRPC.

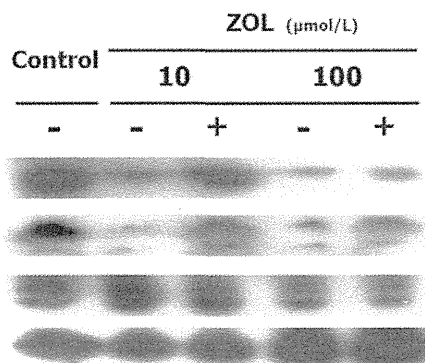


Fig. 6. Effects of ZOL on Ras/MAPK pathway of NE CS cells. We used farnesyl pyrophosphate ammonium salt (FOH), which potentially induces farnesylation of Ras. Ras activity was evaluated by pull down assay, and Erk activity by Western blot assay. As evaluated by pull down assay, 10, and 100 μ mol/L ZOL inhibited Ras activation in NE CS cells, and then the ZOL induced inhibition was reversed by FOH. ZOL inhibited Erk1/2 phosphorylation in NE CS cells as evaluated by Western blot assay.

Somatostatin analogs have been used clinically used to treat NE tumors [23]. SMS and lanreotide, which have high affinity to SSTR2a, have been demonstrated to reduce excessive hormone production and accompanying symptoms from carcinoid tumors and pancreatic endocrine tumors such as glucagonoma, VIPoma and gastrinoma [14]. The anticancer effect may be the result of antiproliferative and apoptotic actions through direct and indirect mechanisms. The direct mechanism is mediated by SSTR on tumor cells, and suppression of secretion of several growth factors such as insulin-like growth factor-1 (IGF-1) may also indirectly inhibit the tumor growth [24–26]. In this study, in spite of the expression of SSTR2a and SSTR5 in our NE carcinoma models, we failed to find significant antiproliferative effects of SMS or SOM monotherapy in vitro or in vivo. In addition, the combination therapy with ZOL did not create a synergistic effect. Although, the exact reason is unclear, both

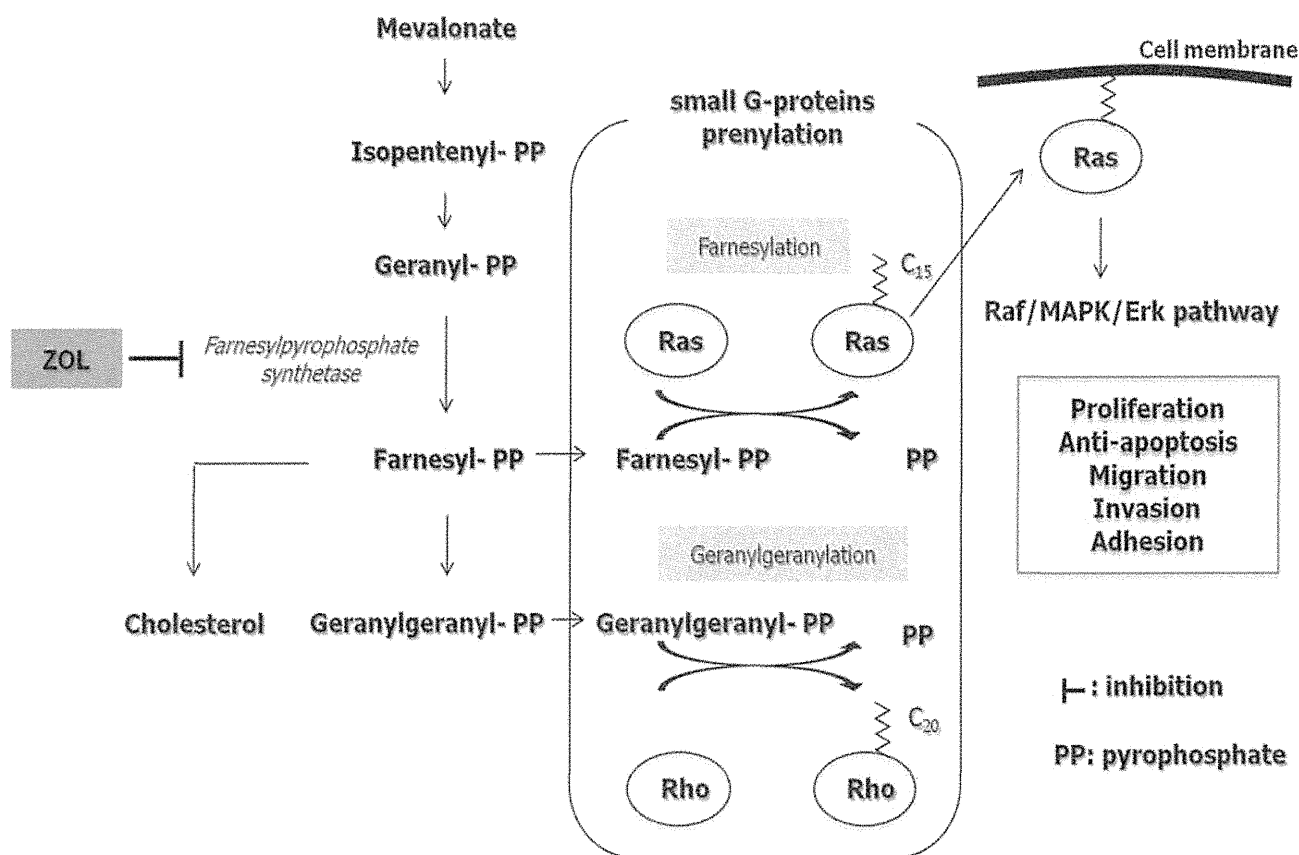


Fig. 7. Schematic representation of the mevalonate pathway and proposed mechanism of anti tumor effects of zoledronic acid in prostatic NE carcinoma.

SMS and SOM might be insufficient to control our NE carcinoma models through autocrine, paracrine and endocrine regulation via SSTRs.

Our results suggest that ZOL induces time- and dose-dependent antiproliferative and apoptotic effects in prostatic NE carcinoma. The observed anticancer activity was exerted at ZOL IC₅₀ levels of from 15.8 to 36.0 $\mu\text{mol/L}$. In addition, the drug reduced migration by 8 hr in vitro even at the 10 $\mu\text{mol/L}$ concentration, and the time and dose did not seem to affect the viability of cells. These effects were caused by disruption of prenylation of Ras proteins as a result of farnesylpyrophosphate synthetase inhibition, disrupting the downstream MAPK/Erk signaling pathway (Fig. 7). Farnesylpyrophosphate synthetase is a key enzyme in the mevalonate pathway, which produces essential lipid molecules such as cholesterol, farnesylpyrophosphate and geranylgeranylpyrophosphate [27]. Small G proteins need prenylation to link to the inner surface of the cell membrane and function in signal translation [28]. Prenylation of small G proteins involves farnesylation, which provides a 15-carbon isoprenoid moiety with Ras, and geranylgeranylation, which provides a 20-carbon isoprenoid moiety with Rap Rac or Rho [27,28]. Ras is the most thoroughly

characterized member of the small G proteins involved in key oncogenic cellular processes such as proliferation, anti-apoptosis, migration, invasion and adhesion (Fig. 7). Therefore, it is anticipated that ZOL disturbing prenylation of Ras will induce multifactorial anticancer effects in cancer cells.

Several studies had shown that ZOL induces apoptosis via impaired prenylation of small G proteins in various cancer cells, including prostate [12,29–31], breast [32,33], myeloma [34], colon [35], and lung cancer cell lines [36]. Caraglia et al. [12] reported the effects of the combination of ZOL and farnesyltransferase inhibitor R115777 on PC3 and DU145 prostate cancer cell lines. These effects paralleled disruption of Ras/MAPK/Erk and Akt survival pathways, which consequently decreased phosphorylation of both mitochondrial bcl-2 and bad proteins, and caspase activation. These findings may support our results indicating that ZOL induced apoptosis of NE cells. Recent studies have shown that impaired geranylgeranylation on other small G proteins such as Rap1 [29,34] and RhoA [32] is also crucial for the association with these apoptotic actions induced by ZOL.

We also demonstrated that ZOL induced cell cycle arrest of the NE carcinoma cells. Both in vitro, and in

vivo, ZOL reduced the numbers of Ki67-positive cells during all active phases of the cell cycle (G1, S, G2, and M). ZOL has been shown to reduce the expression of cyclin D1 and cyclin E in osteosarcoma cells, resulting in a cell cycle block at G1, and S [37]. In addition, experiments using leukemia cells have shown that ZOL can also reduce the expression of cyclin D3 and cyclin B, resulting in a cell cycle block at G2-M [38]. These actions are suggested to occur in a p53-independent manner followed by subsequent apoptosis. Our results indicated that ZOL inhibited the cell cycle of NE cells.

Moreover, we demonstrated that ZOL inhibited migration of NE-CS cells. It decreased the weights of livers having metastatic nodules in castrated NE-10 allografts, which means to suppress liver metastases. Likewise, Hiraga et al. [39] reported that 1 $\mu\text{mol/L}$ ZOL significantly inhibited cell invasion in a breast cancer cell line (4T1/Luc), which consequently led to suppression of liver and bone metastases. Similar results were also observed in prostate cancer cell lines LNCaP, PC3, and DU145 31. In addition, Coxon et al. [40] reported an inhibitory effect of 1 $\mu\text{mol/L}$ ZOL on adhesion to mineralized matrix in PC3, and DU145 cells. Although the exact mechanisms underlying these effects remain unclear, it is suggested that ZOL could inhibit several matrix metalloproteinase or adhesion molecules via impairment of prenylation of small G proteins. It is noteworthy that ZOL also inhibits essential steps for the spread of cancer cells. In addition, recent reports have shown that ZOL indirectly exerts anticancer effects via elevated function of gamma delta T cells [41,42]. It is suggested that accumulation of isopentenyl-pyrophosphate caused by ZOL may be involved in activation of gamma delta T cells [43].

There are some limitations in this study. The NE-10 allograft and the NE-CS cell line were derived from the mouse prostate. The role of human NE cells in human prostate cancer may be different from that of mouse NE cells. In addition, the characteristics of the established cell line, NE-CS, could be different from those of the original NE-10 allograft because cells suitable for survival in vitro were selected during establishment of the cell line. However, there are no ideal human lines for which both in vitro, and in vivo NE carcinoma models are available. In addition, the concentration of ZOL that induced anticancer effects in our experiments was high in comparison to the peak plasma levels ($393 \pm 100 \text{ ng/ml}$) usually achieved by intravenous infusion in patients [44]. Anticancer effects of ZOL might be considered to be exerted basically in bone metastatic lesions in which high concentrations of ZOL are achieved.

In patients with bone metastasis of prostate cancer, ZOL is commonly used for relieving pain and preventing skeletal-related events. This study revealed effects of ZOL on NE cells, potential triggers of prostate cancer leading to CRPC. Regulating the microenvironment between NE cells and prostate cancer cells may result in benefits to patients who do not have clinically detected bone metastasis. We believe that our results support the clinical rationale for earlier proactive use of ZOL, though further studies will be needed to confirm this.

CONCLUSION

We examined the in vitro, and in vivo anti-tumor effects of ZOL and somatostatin analogs (SMS and SOM) on NE carcinoma models. Our results indicate that ZOL, but not SMS or SOM, induces apoptosis and inhibition of proliferation and migration through impaired prenylation of Ras. Our findings support the possibility that ZOL could be used in the early phase for controlling NE cells which may trigger progression of prostate cancer to CRPC.

REFERENCES

1. Jemal A, Bray F, Center MM, Ferlay J, Ward E, Forman D. Global cancer statistics. *CA Cancer J Clin* 2011;61(2):69-90.
2. Heidenreich A, Aus G, Bolla M, Joniau S, Matveev VB, Schmid HP, Zattoni F. EAU guidelines on prostate cancer. *Eur Urol* 2008;53(1):68-80.
3. Debes JD, Tindall DJ. Mechanisms of androgen refractory prostate cancer. *N Engl J Med* 2004;351(15):1488-1490.
4. di Sant'Agnese PA. Neuroendocrine differentiation in prostatic carcinoma: An update. *Prostate Suppl* 1998;8:74-79.
5. Ito T, Yamamoto S, Ohno Y, Namiki K, Aizawa T, Akiyama A, Tachibana M. Up regulation of neuroendocrine differentiation in prostate cancer after androgen deprivation therapy, degree and androgen independence. *Oncol Rep* 2001;8(6):1221-1224.
6. Hirano D, Okada Y, Minei S, Takimoto Y, Nemoto N. Neuroendocrine differentiation in hormone refractory prostate cancer following androgen deprivation therapy. *Eur Urol* 2004;45(5):586-592; discussion 592.
7. Masumori N, Thomas TZ, Chaurand P, Case T, Paul M, Kasper S, Tsukamoto T, Shappell SB, Matusik RJ. A probasin Large T antigen transgenic mouse line develops prostate adenocarcinoma and neuroendocrine carcinoma with metastatic potential. *Cancer Res* 2001;61(5):2239-2249.
8. Masumori N, Tsuchiya K, Tu WH, Lee C, Kasper S, Tsukamoto T, Shappell SB, Matusik RJ. An allograft model of androgen independent prostatic neuroendocrine carcinoma derived from a large probasin promoter T antigen transgenic mouse line. *J Urol* 2004;171(1):439-442.
9. Uchida K, Masumori N, Takahashi A, Itoh N, Tsukamoto T. Characterization of prostatic neuroendocrine cell line established from neuroendocrine carcinoma of transgenic mouse allograft model. *Prostate* 2005;62(1):40-48.

10. Uchida K, Masumori N, Takahashi A, Itoh N, Kato K, Matusik RJ, Tsukamoto T. Murine androgen independent neuroendocrine carcinoma promotes metastasis of human prostate cancer cell line LNCaP. *Prostate* 2006;66(5):536-545.
11. Saad F, Gleason DM, Murray R, Tchekmedyian S, Venner P, Lacombe L, Chin JL, Vinholes JJ, Goas JA, Chen B. A randomized, placebo controlled trial of zoledronic acid in patients with hormone refractory metastatic prostate carcinoma. *J Natl Cancer Inst* 2002;94(19):1458-1468.
12. Caraglia M, Marra M, Leonetti C, Meo G, D'Alessandro AM, Baldi A, Santini D, Tonini G, Bertieri R, Zupi G, Budillon A, Abbruzzese A. R115777 (Zarnestra)/Zoledronic acid (Zometa) cooperation on inhibition of prostate cancer proliferation is paralleled by Erk/Akt inactivation and reduced Bcl 2 and bad phosphorylation. *J Cell Physiol* 2007;211(2):533-543.
13. Patel YC. Somatostatin its receptor, family *Front Neuroendocrinol* 1999;20(3):157-198.
14. Hejna M, Schmidinger M, Raderer M. The clinical role of somatostatin analogs as antineoplastic agents: Much ado about nothing? *Ann Oncol* 2002;13(5):653-668.
15. Reubi JC, Waser B, Schaer JC, Laissue JA. Somatostatin receptor SSTR1 SSTR5 expression in normal and neoplastic human tissues using receptor autoradiography with subtype selective ligands. *Eur J Nucl Med* 2001;28(7):836-846.
16. Halmos G, Schally AV, Sun B, Davis R, Bostwick DG, Plonowski A. High expression of somatostatin receptors and messenger ribonucleic acid for its receptor subtypes in organ confined and locally advanced human prostate cancers. *J Clin Endocrinol Metab* 2000;85(7):2564-2571.
17. Bruns C, Lewis I, Briner U, Meno Tetang G, Weckbecker G. SO M230 a novel somatostatin peptidomimetic with broad somatotropin release inhibiting factor (SRIF) receptor binding and a unique antisecretory profile. *Eur J Endocrinol* 2002;146(5):707-716.
18. Chou TC, Talalay P. Quantitative analysis of dose effect relationships: The combined effects of multiple drugs or enzyme inhibitors. *Adv Enzyme Regul* 1984;22:27-55.
19. Topaly J, Zeller WJ, Fruehauf S. Synergistic activity of the new ABL specific tyrosine kinase inhibitor STI571 and chemotherapeutic drugs on BCR ABL positive chronic myelogenous leukemia cells. *Leukemia* 2001;15(3):342-347.
20. Bok RA, Small EJ. Bloodborne biomolecular markers in prostate cancer development and progression. *Nat Rev Cancer* 2002;2(12):918-926.
21. Jin RJ, Wang Y, Masumori N, Ishii K, Tsukamoto T, Shappell SB, Hayward SW, Kasper S, Matusik RJ. NE 10 neuroendocrine cancer promotes the LNCaP xenograft growth in castrated mice. *Cancer Res* 2004;64(15):5489-5495.
22. Weinstein MH, Partin AW, Veltri RW, Epstein JI. Neuroendocrine differentiation in prostate cancer: Enhanced prediction of progression after radical prostatectomy. *Hum Pathol* 1996;27(7):683-687.
23. Sciarra A, Bosman C, Monti G, Gentile V, Autran Gomez AM, Ciccariello M, Pastore A, Salvatori G, Fattore F, Di Silverio F. Somatostatin analogs and estrogens in the treatment of androgen ablation refractory prostate adenocarcinoma. *J Urol* 2004;172(5 Pt 1):1775-1783.
24. Pawlikowski M, Melen Mucha G. Perspectives of new potential therapeutic applications of somatostatin analogs. *Neuro Endocrinol Lett* 2003;24(1-2):21-27.
25. van der Hoek J, van der Lelij AJ, Feelders RA, de Herder WW, Uitterlinden P, Poon KW, Boerlin V, Lewis I, Krahnke T, Hofland LJ, Lamberts SW. The somatostatin analogue SOM230, compared with octreotide, induces differential effects in several metabolic pathways in acromegalic patients. *Clin Endocrinol (Oxf)* 2005;63(2):176-184.
26. Schmid HA. Pasireotide (SOM230): Development, mechanism of action and potential applications. *Mol Cell Endocrinol* 2008;286(1-2):69-74.
27. Kavanagh KL, Guo K, Dunford JE, Wu X, Knapp S, Ebetino FH, Rogers MJ, Russell RG, Oppermann U. The molecular mechanism of nitrogen containing bisphosphonates as antiosteoporosis drugs. *Proc Natl Acad Sci USA* 2006;103(20):7829-7834.
28. Houglund JL, Fierke CA. Getting a handle on protein prenylation. *Nat Chem Biol* 2009;5(4):197-198.
29. Nogawa M, Yuasa T, Kimura S, Kuroda J, Segawa H, Sato K, Yokota A, Koizumi M, Maekawa T. Zoledronic acid mediates Ras independent growth inhibition of prostate cancer cells. *Oncol Res* 2005;15(1):1-9.
30. Fabbri F, Brigliadori G, Carloni S, Ulivi P, Vannini I, Tesei A, Silvestrini R, Amadori D, Zoli W. Zoledronic acid increases docetaxel cytotoxicity through pMEK and Mcl 1 inhibition in a hormone sensitive prostate carcinoma cell line. *J Transl Med* 2008;6:43.
31. Mani J, Vallo S, Barth K, Makarevic J, Juengel E, Bartsch G, Wiesner C, Haferkamp A, Blaheta RA. Zoledronic acid influences growth, migration and invasive activity of prostate cancer cells in vitro. *Prostate Cancer Prostatic Dis* 2012;15(3):250-255.
32. Denoyelle C, Hong L, Vannier JP, Soria J, Soria C. New insights into the actions of bisphosphonate zoledronic acid in breast cancer cells by dual RhoA dependent and independent effects. *Br J Cancer* 2003;88(10):1631-1640.
33. Ottewell PD, Lefley DV, Cross SS, Evans CA, Coleman RE, Holen I. Sustained inhibition of tumor growth and prolonged survival following sequential administration of doxorubicin and zoledronic acid in a breast cancer model. *Int J Cancer* 2009;126(2):522-532.
34. Guenther A, Gordon S, Tiemann M, Burger R, Bakker F, Green JR, Baum W, Roelofs AJ, Rogers MJ, Gramatzki M. The bisphosphonate zoledronic acid has antimyeloma activity in vivo by inhibition of protein prenylation. *Int J Cancer* 2010;126(1):239-246.
35. Sewing L, Steinberg F, Schmidt H, Goke R. The bisphosphonate zoledronic acid inhibits the growth of HCT 116 colon carcinoma cells and induces tumor cell apoptosis. *Apoptosis* 2008;13(6):782-789.
36. Tannehill Gregg SH, Levine AL, Nadella MV, Iguchi H, Rosol TJ. The effect of zoledronic acid and osteoprotegerin on growth of human lung cancer in the tibias of nude mice. *Clin Exp Metast* 2006;23(1):19-31.
37. Kubista B, Trieb K, Sevelde F, Toma C, Arrich F, Heffeter P, Elbling L, Sutterluty H, Scotlandi K, Kotz R, Micksche M, Berger W. Anticancer effects of zoledronic acid against human osteosarcoma cells. *J Orthop Res* 2006;24(6):1145-1152.
38. Kuroda J, Kimura S, Segawa H, Kobayashi Y, Yoshikawa T, Urasaki Y, Ueda T, Enjo F, Tokuda H, Ottmann OG, Maekawa T. The third generation bisphosphonate zoledronate synergistically augments the anti pH + leukemia activity of imatinib mesylate. *Blood* 2003;102(6):2229-2235.
39. Hiraga T, Williams PJ, Ueda A, Tamura D, Yoneda T. Zoledronic acid inhibits visceral metastases in the 4T1/Luc mouse breast cancer model. *Clin Cancer Res* 2004;10(13):4559-4567.

40. Coxon JP, Oades GM, Kirby RS, Colston KW. Zoledronic acid induces apoptosis and inhibits adhesion to mineralized matrix in prostate cancer cells via inhibition of protein prenylation. *BJU Int* 2004;94(1):164-170.
41. Marten A, Lilienfeld Toal M, Buchler MW, Schmidt J. Zoledronic acid has direct antiproliferative and antimetastatic effect on pancreatic carcinoma cells and acts as an antigen for delta2 gamma/delta T cells. *J Immunother* 2007;30(4):370-377.
42. Sato K, Kimura S, Segawa H, Yokota A, Matsumoto S, Kuroda J, Nogawa M, Yuasa T, Kiyono Y, Wada H, Maekawa T. Cytotoxic effects of gammadelta T cells expanded ex vivo by a third generation bisphosphonate for cancer immunotherapy. *Int J Cancer* 2005;116(1):94-99.
43. Roelofs AJ, Jauhainen M, Monkkonen H, Rogers MJ, Monkkonen J, Thompson K. Peripheral blood monocytes are responsible for gamma delta T cell activation induced by zoledronic acid through accumulation of IPP/DMAPP. *Br J Haematol* 2009;144(2):245-250.
44. Reid IR, Brown JP, Burckhardt P, Horowitz Z, Richardson P, Trechsel U, Widmer A, Devogelaer JP, Kaufman JM, Jaeger P, Body JJ, Brandi ML, Broell J, Di Micco R, Genazzani AR, Feltenberg D, Happ J, Hooper MJ, Ittner J, Leb G, Mallmin H, Murray T, Ortolani S, Rubinacci A, Saaf M, Samsioe G, Verbruggen L, Meunier PJ. Intravenous zoledronic acid in postmenopausal women with low bone mineral density. *N Engl J Med* 2002;346(9):653-661.

Prognostic significance of subtype and pathologic response in operable breast cancer; a pooled analysis of prospective neoadjuvant studies of JBCRG

Katsumasa Kuroi · Masakazu Toi · Shinji Ohno · Seigo Nakamura · Hiroji Iwata · Norikazu Masuda · Nobuaki Sato · Hitoshi Tsuda · Masafumi Kurosumi · Futoshi Akiyama

Received: 17 October 2013 / Accepted: 22 November 2013
© The Japanese Breast Cancer Society 2013

Abstract

Purpose In the past decade, JBCRG has conducted three studies of neoadjuvant chemotherapy which have examined sequential combination of fluorouracil, epirubicin and cyclophosphamide, and docetaxel. The present study is a pooled analysis of these studies performed to determine the prognostic significance of pathologic complete response (pCR) and predictive variables for pCR.

Methods A total of 353 patients were included. pCR was defined as the absence of invasive cancer or only a few remaining isolated cancer cells in the breast (quasi-pCR, QpCR).

Results Disease-free survival (DFS) and overall survival (OS) were not significantly different among studies, and patients who achieved a QpCR had significantly better prognosis (DFS, $p < 0.001$; OS, $p = 0.002$). Patients with triple-negative (TN) tumors had worse prognosis than patients with the other subtypes (DFS, $p = 0.03$; OS, $p = 0.10$). A Cox proportional hazards model showed node-positive, TN, and QpCR were the significant predictors for DFS and OS among study, age, tumor size, nuclear grade, nodal status, subtype, clinical response, and pathologic response (DFS; node-positive, HR = 2.29, $p = 0.001$; TN, HR = 3.39, $p < 0.001$; QpCR, HR = 0.27, $p < 0.001$; OS; node-positive, HR = 3.05,

K. Kuroi
Department of Surgery, Tokyo Metropolitan Cancer and Infectious Diseases Center Komagome Hospital,
3 18 22 Honkomagome, Bunkyo ku, Tokyo 113 8677, Japan

K. Kuroi (✉)
Department of Surgery, Tokyo Metropolitan Komagome Hospital, 3 18 22 Honkomagome, Bunkyo ku, Tokyo 113 8677, Japan
e mail: kurochan@dd.iij4u.or.jp

M. Toi
Department of Surgery (Breast Surgery), Graduate School of Medicine Kyoto University, Kyoto, Japan

S. Ohno
Department of Clinical Oncology, The Clinical Institute of NHO Kyusyu Cancer Center, Fukuoka, Japan

S. Nakamura
Division of Breast Surgical Oncology, Department of Surgery, Showa University School of Medicine, Tokyo, Japan

S. Nakamura
Department of Breast Surgical Oncology, St. Luke's International Hospital, Tokyo, Japan

H. Iwata
Department of Breast Oncology, Aichi Cancer Center Hospital, Aichi, Japan

N. Masuda
Department of Surgery, Breast Oncology, NHO Osaka National Hospital, Osaka, Japan

N. Sato
Department of Breast Oncology, Niigata Cancer Center Hospital, Niigata, Japan

H. Tsuda
Department of Basic Pathology, National Defense Medical College, Saitama, Japan

M. Kurosumi
Department of Pathology, Saitama Cancer Center, Saitama, Japan

F. Akiyama
Department of Pathology, The Cancer Institute of Japanese Foundation for Cancer Research, Tokyo, Japan

$p = 0.003$; TN, HR = 4.92, $p < 0.001$; QpCR, HR = 0.12, $p < 0.001$). In a logistic regression analysis, subtype and clinical response before surgery were the significant predictive variables for QpCR (luminal/Her2-positive, odds ratio (OR) = 4.15, $p = 0.002$; Her2-positive, OR = 6.24, $p < 0.001$; TN, OR = 4.24, $p < 0.001$; clinical response before surgery, OR = 2.41, $p = 0.019$).

Conclusions This study confirmed the prognostic significance of QpCR and nodal status and the predictive and prognostic significance of subtype in neoadjuvant chemotherapy.

Keywords Neoadjuvant chemotherapy · Pathologic response · Subtype · Anthracycline · Taxane

Introduction

Neoadjuvant chemotherapy (NAC) has become part of the standard care for operable breast cancer to increase the chance of breast conservation [1, 2]. NAC also enables us to evaluate tumor response to determine whether ineffective therapy should be discontinued and replaced with an alternative therapy. To date, a sequential anthracycline-containing regimen and taxane are a frequently used regimen, and pathologic complete response (pCR) has predicted the long-term outcome, and is thus regarded as a potential surrogate marker for survival [1, 2]. More recently, however, several studies have demonstrated that the incidence and prognostic impact of pCR could vary among breast cancer subtypes [2–5]. Moreover, as several definitions of pCR have been used, the term pCR has not been applied in a consistent manner [6].

In the past decade, the Japan Breast Cancer Research Group (JBCRG) has conducted three prospective phase II studies of NAC, JBCRG-01, JBCRG-02, and JBCRG-03, and found that 8 cycles of fluorouracil, epirubicin, and cyclophosphamide (FEC), and docetaxel (DOC) were safe, feasible, and effective, and that subtype was predictive for pCR [7–9]. In these studies, pCR was defined as the absence of invasive cancer (ypT0, ypTis) or only a few remaining isolated cancer cells in the breast (near pCR) (quasi-pCR, QpCR) [6, 8–10]. The present study is a pooled analysis of these previous JBCRG studies performed to determine the prognostic significance of QpCR and predictive variables for QpCR.

Patients and methods

Studies

Between 2002 and 2006, JBCRG-01 ($n = 202$), JBCRG-02 ($n = 50$) and JBCRG-03 ($n = 137$) were conducted in

Japan. Details of the individual studies have been described previously [7–9]. All studies were approved by the relevant ethics committees, and all patients provided written informed consent for study participation and data collection. All studies were registered to UMIN (JBCRG-01, C000000011; JBCRG-02, C000000020, C000000320; JBCRG-03, C000000291).

All three studies had comparable main eligibility criteria. The diagnosis of invasive breast cancer was histologically confirmed in all patients by core biopsy. Female patients needed to have a measurable breast tumor of at least 1 cm. Locally advanced or inflammatory breast cancer was not eligible. Prior to surgery, 4 cycles of fluorouracil 500 mg/m², epirubicin 100 mg/m², and cyclophosphamide 500 mg/m², q3w followed by 4 cycles of DOC 75 mg/m², q3w were administered in JBCRG-01, and the dose of DOC was increased to 100 mg/m² in JBCRG-02 [7, 8]. In JBCRG-03, FEC and DOC were administered in reverse order from JBCRG-01 [9]. Patients with hormone receptor (HR)-positive tumors were encouraged to receive adjuvant endocrine treatment for at least 5 years, and adjuvant radiation therapy was recommended for patients who underwent breast-conserving surgery. No patients received trastuzumab as a part of NAC; however, after the approval of adjuvant use of trastuzumab in 2008, patients could receive trastuzumab for 1 year, if indicated.

Assessment of response

Clinical tumor assessments were performed at each institute within 4 weeks before initiation of NAC, after completion of the first 4 cycles of chemotherapy and before surgery according to the modified Response Evaluation Criteria in Solid Tumors (RECIST) guideline. Clinical examinations were based on palpable changes in tumor size in combination with mammography, ultrasonography, computed tomography (CT), and magnetic resonance imaging (MRI). Pathologic response was independently evaluated by a blinded central review committee according to the criteria of the Japanese Breast Cancer Society [6, 10], and near pCR was defined as extremely high grade marked changes approaching a complete response, with a few remaining isolated cancer cells. For an assessment of QpCR, multiple tumor sections were examined, and cyto-keratin immunostaining was performed to confirm the presence of residual cancer cells, if required.

Assessment of HR and Her2

Estrogen receptor (ER) status and progesterone receptor (PgR) status were determined by immunohistochemistry at each institute and, in general, tumors with >10 %

positively stained tumor cells were classified as positive for ER and PgR. Her2 status was also determined at each institute by immunohistochemistry or by fluorescence in situ hybridization (FISH) analysis. Her2-positive tumors were defined as 3+ on immunohistochemistry or as positive by FISH. Subtypes were classified into luminal (ER-positive and/or PgR-positive, Her2-negative), luminal/Her2-positive (ER-positive and/or PgR-positive, Her2-positive), Her2-positive (ER-negative, PgR-negative, Her2-positive), and triple-negative (TN) (ER-negative, PgR-negative, Her2-negative).

Statistical analysis

Individual patient data regarding baseline characteristics, histopathological results at diagnosis and surgery, and follow-up was extracted for this pooled analysis from the original databases. Only patients who received at least one cycle of systemic chemotherapy were included. Patients were excluded due to missing data for ER, PgR,

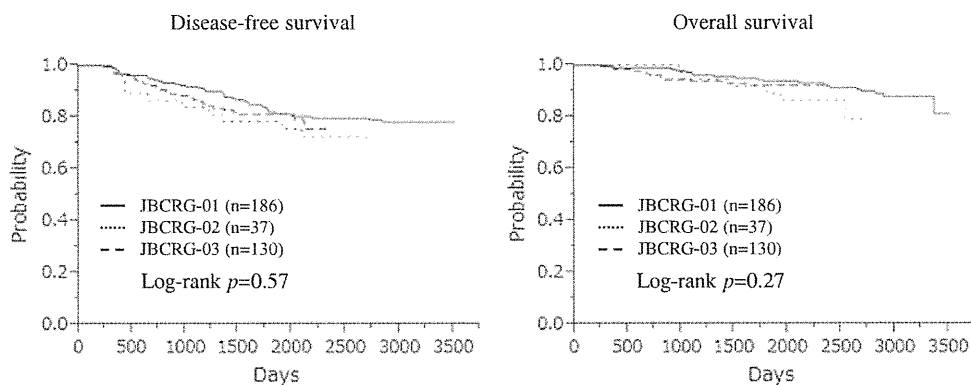
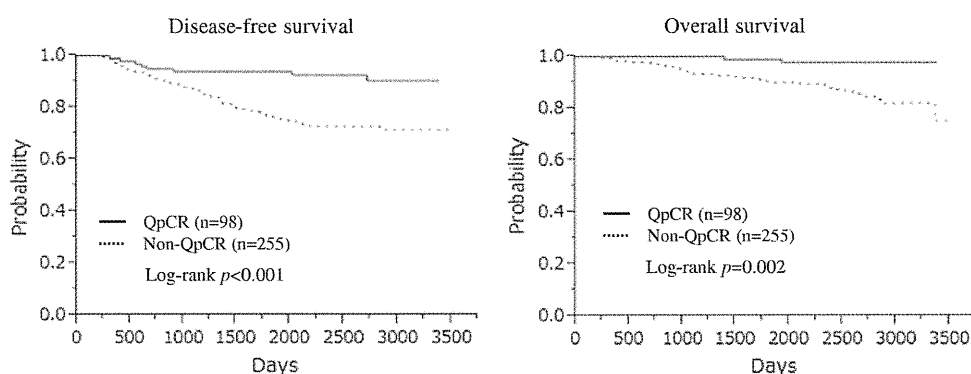
Her2, or surgery and due to ineligibility or withdrawal of consent.

Comparisons between groups were performed with the chi square test or Fisher's exact test for proportions and Wilcoxon test for continuous variables. Disease-free survival (DFS) and overall survival (OS) were calculated from the date of initiation of NAC to the date of last follow-up, recurrence, second cancers, contralateral breast cancers, or death by using the Kaplan Meier method. Comparisons were made by using the log-rank test. Hazard ratios (HzRs), 95 % confidence interval (CI), and corresponding *p* values were calculated by using the Cox proportional hazards model. Factors associated with QpCR were assessed by using univariate analysis, and odds ratios (ORs), 95 % CI, and corresponding *p* values were assessed by using logistic regression analysis. In multivariate analysis, variables were chosen on the basis of the goodness of fit. Statistical analyses were performed with JMP (version 10, SAS Institute Inc.), and *p* < 0.05 was considered statistically significant.

Table 1 Patient characteristics

	JBCRG 01 (2002.6 2004.6)	JBCRG 02 (2004.8 2006.7)	JBCRG 03 (2005.10 2006.10)	<i>p</i> value
No	186	37	130	
Median age (range)	46 (28 60)	45 (30 57)	46 (24 62)	0.62
Tumor size				
≤3 cm	82	19	45	0.11
>3 cm	104	18	85	
Nuclear grade				
Grade 1	34	13	22	0.32
Grade 2	43	13	46	
Grade 3	39	8	29	
Unknown	70	3	33	
Nodal status				
n0	109	22	79	0.93
n+	77	15	51	
Subtype				
Luminal	113	22	71	0.91
Luminal/Her2 positive	15	3	16	
Her2 positive	21	4	15	
Triple negative	37	8	28	
RR (%)				
After the first half of NAC	59.7	59.5	62.3	0.88
Before surgery	74.2	67.6	75.4	0.24
Quasi pCR rate (%)	25.3	35.1	29.1	0.43
Adjuvant therapy				
None	70	16	45	0.62
Endocrine	111	17	72	0.29
Trastuzumab	4	3	10	0.042

CR complete response, NAC neoadjuvant chemotherapy, pCR pathologic complete response, RR response rate

Fig. 1 Prognostic impact of study**Fig. 2** Prognostic impact of pathologic response

Results

A total of 353 patients were included in this analysis among 389 patients who received sequential FEC and DOC as NAC (Table 1). With a median follow-up of 2274 days, 76 DFS events (21 %) and 36 deaths (10 %) occurred. There were no significant differences among studies in terms of patient age at time of study entry, menopausal status, tumor size, nuclear grade, nodal status, subtype, clinical response (after the first half of NAC, before surgery), and pathological response. Ki-67 was not available in the majority of patients and nuclear grade was not assessed in 106 patients (30 %). Among the 353 patients, 206 (58 %) were luminal, 34 (10 %) were luminal/Her2-positive, 40 (11 %) were Her2-positive, and 73 (21 %) were TN. According to protocol and practice guidelines, 200 patients received adjuvant endocrine therapy (no significant difference among studies), and 17 patients received postoperative adjuvant trastuzumab for 1 year. There was a significant increase in the use of adjuvant trastuzumab in JBCRG-02 and JBCRG-03 as compared to JBCRG-01 ($p = 0.042$).

DFS and OS were not significantly different among the three studies (DFS, $p = 0.57$; OS, $p = 0.27$) (Fig. 1). On the other hand, as shown in Fig. 2, patients who achieved QpCR had significantly improved survivals compared to

patients without QpCR (DFS, $p < 0.001$; OS, $p = 0.002$), and patients with QpCR experienced greater DFS and OS as compared to patients without QpCR in JBCRG-01, and patients with QpCR showed a trend towards greater DFS and OS in JBCRG-02 and JBCRG-03 (DFS; JBCRG-01, $p < 0.001$, JBCRG-02, $p = 0.07$, JBCRG-03, $p = 0.46$; OS; JBCRG-01, $p < 0.001$, JBCRG-02, $p = 0.28$, JBCRG-03, $p = 0.17$) (Fig. 3). The types of events was not different among studies (data not shown). Patients with TN tumors had worse survivals than patients with luminal, luminal/Her2-positive, and Her2-positive tumors (DFS, $p = 0.031$; OS, $p = 0.10$) (Fig. 4). When DFS and OS according to subtype was analyzed separately for patients with or without QpCR, patients who achieved QpCR had significantly improved DFS as compared to patients without QpCR in luminal, luminal/Her2-positive, and Her2-positive tumors ($p = 0.022$, $p = 0.028$, $p = 0.003$, respectively), and those who achieved QpCR had significantly improved OS compared to those without QpCR in Her2-positive and TN tumors ($p = 0.024$, $p = 0.031$, respectively) (Fig. 5). There was a trend towards better prognosis in patients with QpCR as compared to those without QpCR in DFS for patients with TN tumors ($p = 0.11$) and in OS for patients with luminal or luminal/Her2-positive tumors (luminal, $p = 0.09$; luminal/Her2-positive, $p = 0.16$). The Cox proportional hazards model

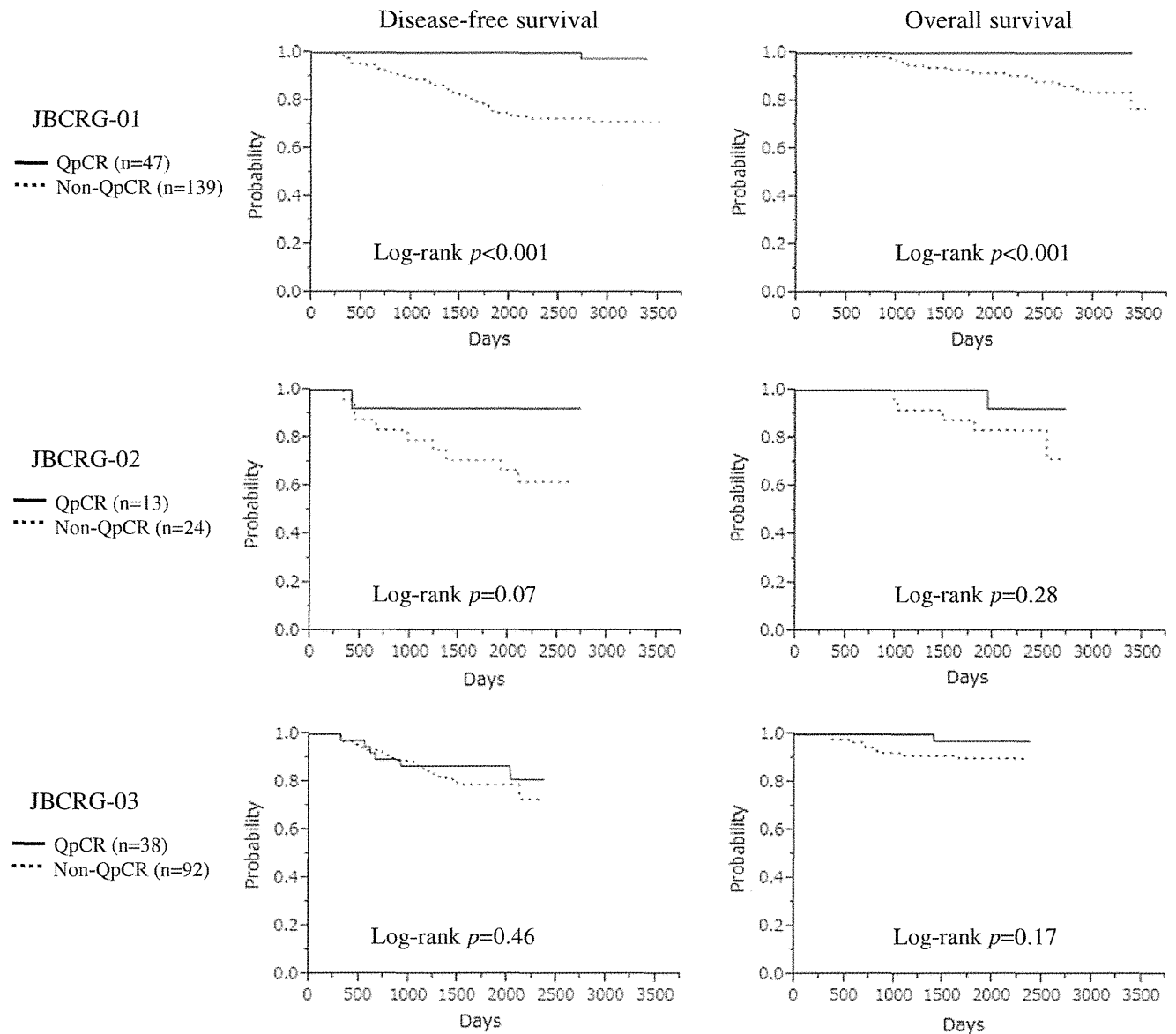
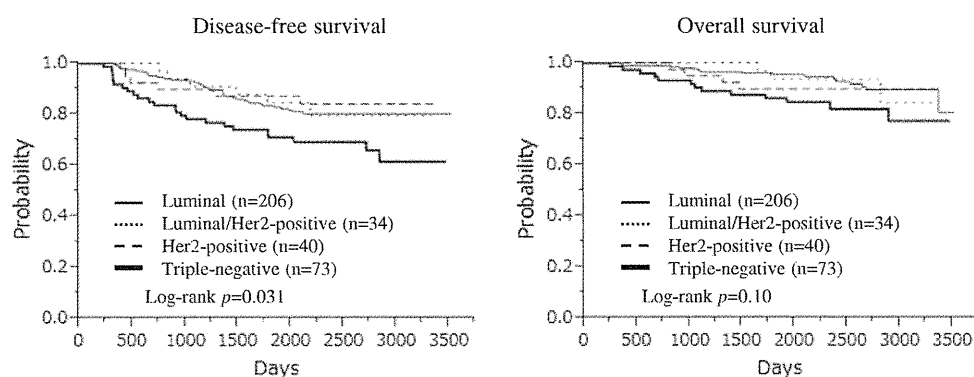


Fig. 3 Prognostic impact of pathologic response according to studies

showed node-positive, TN, and QpCR were the significant predictors for DFS and OS among study, age, tumor size, nuclear grade, nodal status, subtype, clinical response, and pathologic response (DFS; node-positive, $\text{HzR} = 2.29$, $p = 0.001$; TN, $\text{HzR} = 3.39$, $p < 0.001$; QpCR, $\text{HzR} = 0.27$, $p < 0.001$; OS; node-positive, $\text{HzR} = 3.05$, $p = 0.003$; TN, $\text{HzR} = 4.92$, $p < 0.001$; QpCR, $\text{HzR} = 0.12$, $p < 0.001$) (Tables 2, 3).

As shown in Table 4, luminal/Her2-positive, Her2-positive and TN tumors showed significantly higher QpCR rates than luminal tumors (41.2, 52.5, 42.5, 15.5 %, respectively) ($p < 0.001$), and the clinical response was

also significantly associated with QpCR in univariate analysis (clinical response after the first half of NAC, $p < 0.001$; clinical response before surgery, $p < 0.001$). When logistic regression analysis was performed to examine which variables among study, age, tumor size, nuclear grade, subtype, and clinical response were associated with QpCR, subtype (luminal/Her2-positive, Her2-positive, TN), and clinical response before surgery were significant predictive variables for QpCR (luminal/Her2-positive, $\text{OR} = 4.15$, $p = 0.002$; Her2-positive, $\text{OR} = 6.24$, $p < 0.001$; TN, $\text{OR} = 4.24$, $p < 0.001$, clinical response before surgery, $\text{OR} = 2.41$, $p = 0.019$) (Table 5).

Fig. 4 Prognostic impact of subtypes

Discussion

This is, to the best of our knowledge, the largest individual patient-based pooled analysis of the prognostic significance of QpCR and the predictive variables for QpCR in prospective studies of neoadjuvant anthracycline-taxane-based chemotherapy. In a similar study, von Minckwitz et al. [3] demonstrated that when pCR was defined as no invasive and no in situ residuals in breast and nodes (ypT0ypN0), the pathologic response could best discriminate between patients with favorable and unfavorable outcomes and was a suitable surrogate end point for patients with luminal B/Her2-negative, Her2-positive and TN tumors, but not for patients with luminal A or luminal B/Her2-positive tumors (irrespective of trastuzumab treatment). In addition, in the meta-analysis of a working group known as the Collaborative Trials in Neoadjuvant Breast Cancer (CTNeoBC) [4], pCR was uncommon in patients with low-grade HR-positive tumors, and pCR (ypT0/isypN0) had prognostic impact in patients with HR-positive-high-grade, HR-positive-Her2-positive, Her2-positive, and TN tumors. Consistent with these studies, we found that pathologic response as well as subtype (i.e., TN) has prognostic significance. In addition, the prognostic significance of QpCR was dependent on subtypes; however, the beneficial effect of QpCR on DFS in luminal and luminal-Her2-positive tumors might be attributed to 8 cycles of NAC, as longer treatment was found to increase pCR rates in HR-positive tumors, irrespective of Her2 status [5].

In the present study, we included near pCR to pCR to ensure consistency among the studies. In this respect, it should be noted that residual invasive diseases (RD) after NAC include a broad range of actual responses from near pCR to frank resistance, and QpCR used in the present study differs from the other studies including focal RD for pCR in the extent of RD [3, 11, 12]. For example, in the former study [3], up to 5 mm of RD was considered as focal, and it was found that focal RD was associated with increased relapse risk, while we strictly limited near pCR to only a few remaining isolated cancer cells [3, 11]. It is

noteworthy that, in the study by Symmans et al. [13], when pathologic responses were subdivided into residual cancer burden (RCB)-0 (ypstage0), RCB-1 (minimal RD), RCB-II (moderate RD) and RCB-III (extensive RD) by calculating RCB as a continuous variable from the primary tumor dimensions, cellularity of the tumor bed, and the number and size of nodal metastases, patients with RCB-I had the same 5-year prognosis as patients with RCB-0. Thus, the inclusion of RCB-1 or near pCR as defined in this study would expand the subset of patients who could be identified as having benefited from NAC [13].

In addition to pathologic response, nodal status was an independent prognostic variable in this study. This finding is consistent with the study of Bear et al. [14] demonstrating that pathologic nodal status was a strong predictor of survival irrespective of pathologic response to the breast. On the other hand, the prognostic impact of QpCR was statistically significant in JBCRG-01, but not in JBCRG-02 and JBCRG-03. One plausible explanation of this difference seems to be due to the adjuvant use of trastuzumab, as more patients received trastuzumab as adjuvant therapy in JBCRG-02 and JBCRG-03 than JBCRG-01. On the other hand, we could not completely exclude another possibility that the sequence of FEC and DOC could affect the survival. However, so far, no strategy has been found to be clearly superior to the others in patients with operable breast cancer [1]. In addition, the potential limitations of the present study should be addressed. We could not divide luminal A tumors and luminal B/Her2-negative tumors; the majority of tumors were HR-positive; the sample size of patients with Her2-positive or TN tumors was small; and the limited number of events could affect the result. Nevertheless, the results of the present study as a whole are consistent with the previous reports in that the prognostic significance of pCR varies according to subtype [3, 4].

Moreover, we found that subtype (i.e., not luminal) was predictive of QpCR. This result is consistent with the meta-analysis by Houssami et al. [15] demonstrating an independent association between subtype and pCR. In that meta-analysis, OR for pCR was highest for TN and HR-

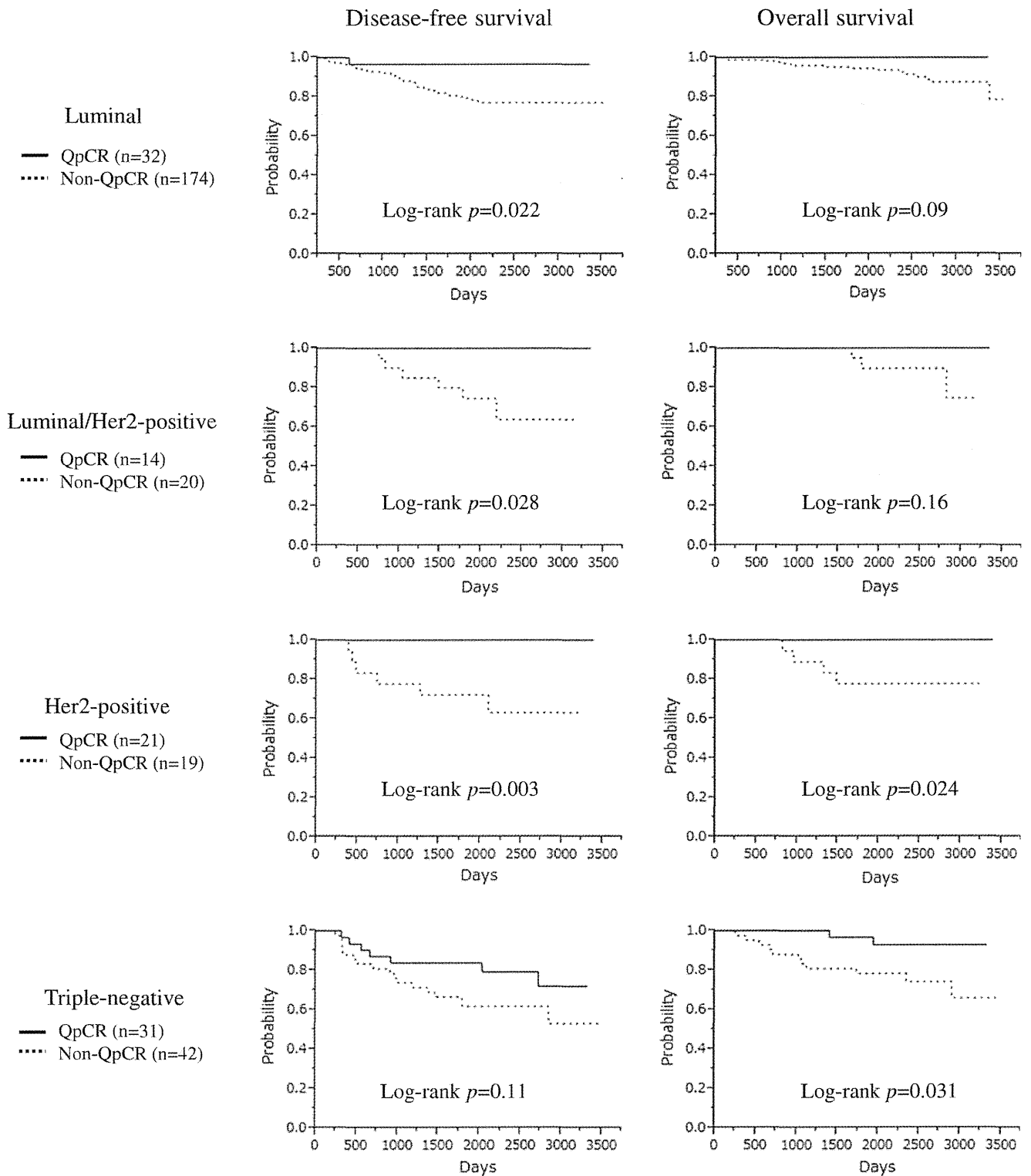


Fig. 5 Prognostic impact of pathologic response according to subtypes

negative/Her2-positive tumors, and in Her2-positive tumors there was an influential effect on achieving pCR through inclusion of Her2-directed therapy with NAC. The significance of simultaneous anti-Her2 treatment with NAC

was also indicated by the Neoadjuvant Herceptin (NOAH) trial [16]. It is also demonstrated that patients with TN tumors have increased pCR rates as compared to non-TN tumors, and patients with pCR have excellent and

Table 2 Multivariate analysis for disease free survival (Cox proportional hazards model)

Variables	HzR	95 % CI	<i>p</i> value
Study			
JBCRG 02	2.09	0.95 4.25	0.07
JBCRG 03	1.31	0.76 2.21	0.32
Age	1.00	0.97 1.03	0.86
Tumor size			
>3 cm	1.19	0.73 1.98	0.48
Nuclear grade			
Grade 3	1.31	0.66 2.55	0.43
Nodal status			
Node positive	2.29	1.40 3.81	0.001
Subtype			
Luminal/Her2 positive	1.62	0.60 3.73	0.32
Her2 positive	1.33	0.48 3.12	0.55
Triple negative	3.39	1.82 6.19	<0.001
Clinical response (CR, PR)			
After the first half of NAC	0.74	0.44 1.27	0.27
Before surgery	0.88	0.48 1.50	0.56
Pathological response			
Quasi pCR	0.27	0.11 0.56	<0.001

CI confidence interval, *CR* complete response, *HzR* hazard risk, *NAC* neoadjuvant chemotherapy, *PR* partial response, *pCR* pathologic complete response

comparable survival, but those without pCR have significantly worse survival if they have TN tumors as compared to non-TN tumors [3, 17]. Similarly, patients with TN tumors had worse survival compared with the others in the present study. In addition, we failed to find statistically significant improvement of DFS by achieving QpCR in patients with TN tumors, and probability of OS tended to decrease with time. Thus, high QpCR rates obtained in patients with TN tumors do not appear to have a meaningful effect on the prognosis of the entire group of patients with TN tumors, and it is conceivable to consider that the worse survival of patients with TN tumors is primarily determined by the worse survival of patients with RD after NAC [17]. These findings indicate the necessity of an individualized approach for preoperative treatment according to subtype or RD after NAC to improve the outcomes of patients receiving NAC [5]. To address these issues, JBCRG is conducting several phase II studies of neoadjuvant-endocrine treatment in patients with HR-positive/Her2-negative tumors and an exploratory randomized phase II study of dual-Her2 blockage therapy (trastuzumab and lapatinib) in Her2-positive operable breast cancer (JBCRG-16/NeoLaTH) [18, 19]. In addition, an international collaborating randomized phase III study is now investigating whether or not capecitabine improves

Table 3 Multivariate analysis for overall survival (Cox proportional hazards model)

Variables	HzR	95 % CI	<i>p</i> value
Study			
JBCRG 03	2.85	0.92 7.81	0.07
JBCRG 02	1.42	0.57 3.42	0.44
Age	0.98	0.94 1.03	0.45
Tumor size			
>3 cm	2.03	0.98 4.54	0.06
Nuclear grade			
Grade 3	1.07	0.39 2.81	0.89
Nodal status			
Node positive	3.05	1.47 6.63	0.003
Subtype			
Luminal/Her2 positive	2.73	0.60 9.08	0.17
Her2 positive	3.31	0.88 10.19	0.07
Triple negative	4.92	2.07 11.42	<0.001
Clinical response (CR, PR)			
After the first half of NAC	0.76	0.34 1.71	0.50
Before surgery	0.55	0.25 1.26	0.16
Pathologic response			
Quasi pCR	0.12	0.02 0.43	<0.001

CI confidence interval, *CR* complete response, *HzR* hazard risk, *n+* node positive, *NAC* neoadjuvant chemotherapy, *PR* partial response, *pCR* pathologic complete response

the outcome in patients with Her2-negative tumors who have RD after NAC (JBCRG-04/CREATE-X) [18, 19].

In addition, this study demonstrated the predictive impact of clinical response before surgery on QpCR by logistic analysis. This finding is consistent with the finding of JBCRG-01, indicating that clinical response was an independent predictive variable for QpCR [7], but is in contrast to the findings of JBCRG-03, in which clinical response was not a significant predictive factor. Although the inconsistency might partially be due to the lack of a standardized method to evaluate clinical response, it should be noted that current imaging techniques may underestimate the biological or pathologic tumor response, as these are primarily based on anatomic information only (tumor size). Therefore, it will be important to identify accurate methods for monitoring early treatment response in order to maximize treatment effectiveness and minimize treatment toxicity without benefit [2]. In this respect, a quantitative contrast-enhanced MRI and [F-18] fluorodeoxyglucose positron emission tomography (FDG PET) might be helpful to identify RD and to predict pCR [2, 20, 21]. Further study is needed to better characterize the response to NAC.

In conclusion, this pooled analysis confirmed the prognostic significance of QpCR in patients who received

Table 4 Predictive variables for QpCR by univariate analysis

Variables	QpCR	Non QpCR	<i>p</i> value
Study			
JBCRG 01	47 (25.3 %*)	139	
JBCRG 02	13 (35.1 %)	24	0.43
JBCRG 03	38 (29.2 %)	92	
Median age (range)			
Tumor size			
≤3 cm	47.5 (29 60)	46 (24 62)	0.57
>3 cm	43 (26.6 %)	103	0.55
>3 cm	55 (29.5 %)	152	
Nuclear grade			
Grade 3	25 (32.9 %)	51	0.18
Grade 2, 1	42 (24.6 %)	129	
Subtype			
Luminal	32 (15.5 %)	174	
Luminal/Her2 positive	14 (41.2 %)	20	<0.001
Her2 positive	21 (52.5 %)	19	
Triple negative	42 (42.5 %)	42	
Clinical response (response rate)			
After the first half of NAC			
SD, PD	29 (20.9 %)	145	0.018
CR, PD	69 (32.2 %)	110	
Before surgery			
SD, PD	15 (16.9 %)	74	0.023
CR, PD	82 (31.4 %)	179	

CR complete response, NAC neoadjuvant chemotherapy, PD progressive disease, PR partial response, pCR pathologic complete response, SD stable disease

* QpCR rate

Table 5 Predictive variables for QpCR by logistic regression analysis

Variables	OR	95 % CI	<i>p</i> value
Study			
JBCRG 02	2.11	0.87 5.05	0.10
JBCRG 03	1.22	0.69 2.17	0.50
Age			
Age	1.01	0.97 1.04	0.65
Tumor size			
>3 cm	0.68	0.39 1.20	0.19
Nuclear grade			
Grade 3	0.70	0.33 1.42	0.32
Subtype			
Luminal/Her2 positive	4.15	1.75 9.86	0.002
Her2 positive	6.24	2.76 14.48	<0.001
Triple negative	4.24	2.14 8.54	<0.001
Clinical response (CR, PR)			
After the first half of NAC			
After the first half of NAC	1.35	0.74 2.50	0.32
Before surgery			
Before surgery	2.41	1.15 5.27	0.019

CI confidence interval, CR complete response, NAC neoadjuvant chemotherapy, OR odds ratio, PR partial response

sequential FEC and DOC regimens as NAC. The QpCR rate was high in patients with luminal/Her2-positive, Her2-positive, and TN tumors as compared to luminal tumors; however, the survival of patients with TN tumors was inferior. This study underscores the significance of a subtype-based, individualized approach for NAC.

Acknowledgments The JBCRG 01 study was supported by the Osaka Cancer Research Foundation and the Advanced Clinical Research Organization; JBCRG 02 and JBCRG 03 studies were supported by the Advanced Clinical Research Organization. The authors gratefully thank the patients who participated in the JBCRG 01, JBCRG 02, and JBCRG 03 studies. The authors also thank Mrs Kiyomi Kashiwa and Mrs Aya Maruyama for their support and data management.

Conflict of interest The authors declare that they have no conflicts of interest to disclose.

References

- Kaufmann M, Hortobagyi GN, Goldhirsch A, Scholl S, Makris A, Valagussa P, et al. Recommendations from an international expert panel on the use of neoadjuvant (primary) systemic treatment of operable breast cancer: an update. *J Clin Oncol.* 2006;24:1940-9.
- Kaufmann M, von Minckwitz G, Bear HD, Buzdar A, McGale P, Bonnefoi H, et al. Recommendations from an international expert panel on the use of neoadjuvant (primary) systemic treatment of operable breast cancer: new perspectives 2006. *Ann Oncol.* 2007;18:1927-34.
- von Minckwitz G, Untch M, Blohmer JU, Costa SD, Eidtmann H, Fasching PA, et al. Definition and impact of pathologic complete response on prognosis after neoadjuvant chemotherapy in various intrinsic breast cancer subtypes. *J Clin Oncol.* 2012;30:1796-804.
- Cortazar P, Zhang L, Untch M, Mehta K, Costantino J, Wolmark N, et al. Meta analysis results from the collaborative trials in neoadjuvant breast cancer (CTNeoBC) S1 11. *Cancer Res.* 2012;72.
- von Minckwitz G, Untch M, Nuesch E, Loibl S, Kaufmann M, Kummel S, et al. Impact of treatment characteristics on response of different breast cancer phenotypes: pooled analysis of the German neoadjuvant chemotherapy trials. *Breast Cancer Res Treat.* 2011;125:145-56.
- Kuroi K, Toi M, Tsuda H, Kurosumi M, Akiyama F. Issues in the assessment of the pathologic effect of primary systemic therapy for breast cancer. *Breast Cancer.* 2006;13:38-48.
- Toi M, Nakamura S, Kuroi K, Iwata H, Ohno S, Masuda N, et al. Phase II study of preoperative sequential FEC and docetaxel predicts of pathological response and disease free survival. *Breast Cancer Res Treat.* 2008;110:531-9.
- Nakamura S, Masuda S, Iwata H, Toi M, Kuroi K, Kurosumi M, et al. Phase II trial of fluorouracil, epirubicin, cyclophosphamide (FEC) followed by docetaxel 100 mg/m² in primary operable breast cancer JBCRG02. *Jpn J Breast Cancer.* 2008;23:111-7.
- Iwata H, Sato N, Masuda N, Nakamura S, Yamamoto N, Kuroi K, et al. Docetaxel followed by fluorouracil/epirubicin/cyclophosphamide as neoadjuvant chemotherapy for patients with primary breast cancer. *Jpn J Clin Oncol.* 2011;41:867-75.
- Kurosumi M, Akashi Tanaka S, Akiyama F, Komoike Y, Mukai H, Nakamura S, et al. Histopathological criteria for assessment of therapeutic response in breast cancer (2007 version). *Breast Cancer.* 2008;15:5-7.

11. Sataloff DM, Mason BA, Prestipino AJ, Seinige UL, Lieber CP, Baloch Z. Pathologic response to induction chemotherapy in locally advanced carcinoma of the breast: a determinant of outcome. *J Am Coll Surg*. 1995;180:297-306.
12. Sinn HP, Schmid H, Junkermann H, Huober J, Leppien G, Kaufmann M, et al. Histologic regression of breast cancer after primary (neoadjuvant) chemotherapy. *Geburtshilfe Frauenheilkd*. 1994;54:552-8.
13. Symmans WF, Peintinger F, Hatzis C, Rajan R, Kuerer H, Valero V, et al. Measurement of residual breast cancer burden to predict survival after neoadjuvant chemotherapy. *J Clin Oncol*. 2007;25:4414-22.
14. Bear HD, Anderson S, Smith RE, Geyer CE Jr, Mamounas EP, Fisher B, et al. Sequential preoperative or postoperative docetaxel added to preoperative doxorubicin plus cyclophosphamide for operable breast cancer: National Surgical Adjuvant Breast and Bowel Project Protocol B 27. *J Clin Oncol*. 2006;24:2019-27.
15. Houssami N, Macaskill P, von Minckwitz G, Marinovich ML, Mamounas E. Meta analysis of the association of breast cancer subtype and pathologic complete response to neoadjuvant chemotherapy. *Eur J Cancer*. 2012;48:3342-54.
16. Gianni L, Eiermann W, Semiglazov V, Manikhas A, Lluch A, Tjulandin S, et al. Neoadjuvant chemotherapy with trastuzumab followed by adjuvant trastuzumab versus neoadjuvant chemotherapy alone, in patients with HER2 positive locally advanced breast cancer (the NOAH trial): a randomised controlled superiority trial with a parallel HER2 negative cohort. *Lancet*. 2010;375:377-84.
17. Liedtke C, Mazouni C, Hess KR, Andre F, Tordai A, Mejia JA, et al. Response to neoadjuvant therapy and long term survival in patients with triple negative breast cancer. *J Clin Oncol*. 2008;26:1275-81.
18. Ohno S, Kuroi K, Toi M. An overview of the Japan Breast Cancer Research Group (JBCRG) activities. *Breast Cancer*. 2013 Mar 15. (Epub ahead of print).
19. Kuroi K, Kashiwa K, Toi M, Nakamura S, Iwata H, Ohno S, et al. Japan Breast Cancer Research Group (JBCRG). *Clin Oncol*. 2010;6:360-8.
20. Manton DJ, Chaturvedi A, Hubbard A, Lind MJ, Lowry M, Maraveyas A, et al. Neoadjuvant chemotherapy in breast cancer: early response prediction with quantitative MR imaging and spectroscopy. *Br J Cancer*. 2006;94:427-35.
21. Rousseau C, Devillers A, Sagan C, Ferrer L, Bridji B, Campion L, et al. Monitoring of early response to neoadjuvant chemotherapy in stage II and III breast cancer by [18F]fluorodeoxyglucose positron emission tomography. *J Clin Oncol*. 2006;24:5366-72.